





## Continuous epoxidation of used cooking oils using an automated slug-flow millireactor<sup>☆</sup>

Juliana Cárdenas<sup>a,b</sup>, Benjamin Katryniok<sup>b</sup>, Marcia Araque-Marin<sup>b</sup>, Wei-Hsin Hsu<sup>c</sup> , Peter H. Seeberger<sup>c</sup>, Jose Dangelad-Flores<sup>c</sup>, Alvaro Orjuela<sup>a,\*</sup> 

<sup>a</sup> Department of Chemical and Environmental Engineering, Universidad Nacional de Colombia 111321 Bogotá D.C., Colombia

<sup>b</sup> Unité de Catalyse et Chimie du Solide, Université de Lille, Cité Scientifique - CS2004859651 Villeneuve d'Ascq Cedex, Lille, France

<sup>c</sup> Department of Biomolecular Systems, Max Planck Institute of Colloids and Interfaces, Am Mühlenberg 1, 14476 Potsdam, Germany

### ARTICLE INFO

#### Keywords:

Used cooking oil  
Slug-flow  
Millireactor  
Automation  
Process intensification  
Epoxidation

### ABSTRACT

This study describes the development of an automated experimental platform designed for the continuous epoxidation of used cooking oils (UCOs) in slug-flow millireactors. This system transforms UCOs into high-value, second-generation oleochemicals, employing an intensified process, ensuring reproducibility, high yields, and enhanced productivity. The epoxidation was conducted via Prilezhaev reaction using H<sub>2</sub>O<sub>2</sub> as an oxidizing agent, peracetic acid as an oxygen carrier, and H<sub>2</sub>SO<sub>4</sub> as a catalyst. Different vegetable oils were tested to assess the impact of unsaturation content and oil properties on the process performance, and it was found that viscosity had a high effect on the hydrodynamic patterns within the reactor and that specific operating conditions were required to reach slug flows with each feedstock. Then, preliminary experiments with UCO yielded suitable operating conditions to ensure a proper slug flow regime. It was found that the high content of polar compounds in UCO had a significant impact in the hydrodynamics of the reactor because those components induce coalescence with the aqueous phase. Thus, the levels of polar components and moisture in UCO can indicate its suitability for further epoxidation in the slug-flow reactor and the necessity for pretreatment. Subsequently, an experimental simplex evolutionary optimization was deployed to verify a selectivity towards oxirane groups > 80 %, with conversions up to 86 % and yields up to 73 %. The optimal operating conditions were 77.4 °C, an H<sub>2</sub>O<sub>2</sub> to oil ratio of 0.84:1, an acid to oil ratio of 0.32:1, and a residence time of 22.7 min. Under these conditions, a conversion of 82 %, selectivity of 86 %, and productivity of 0.75 kg OO·m<sup>-3</sup>·min<sup>-1</sup> were achieved, and the corresponding epoxidized UCO had an oxirane oxygen content of 4.02 wt%.

### 1. Introduction

The chemical industry has increasingly focused on researching and developing more efficient, cost-effective, and environmentally friendly processes to exploit renewable feedstocks in recent years. This shift is driven by the growing societal demand for sustainable products that can be obtained through circular economy approaches. In this context, used cooking oils (UCOs) have emerged as a prominent second-generation raw material that can be used for the production of a large variety of oleochemicals [1,2,3,4]. The exploitation of UCOs helps mitigate the economic and environmental impacts caused by their mismanagement and enables the harnessing of globally available second-generation food waste. After proper pretreatment [5], UCOs can be transformed into

biofuels (e.g. biodiesel, green diesel, green jet) and also a large variety of high value-added specialty oleochemicals, thus making them a key factor in the pursuit of a truly sustainable oleochemical industry.

Despite its potential, the use of UCOs as oleochemical feedstock faces several challenges including the variable fatty acid profiles in the triglycerides from the various cooking oils and fats employed in food processing [6,7], as well as the significant amount of impurities resulting from chemical degradation and contamination during use or handling [8,9,10]. Consequently, UCOs display considerable heterogeneity in their physicochemical properties, suggesting that alongside pretreatment, source separation practices might be necessary to provide suitable feedstocks for specific oleochemical applications [5,9]. This could lead to increased costs and complexities for UCOs management and supply

<sup>☆</sup> This article is part of a special issue entitled: 'Sustainable Chemical Engineering' published in Chemical Engineering Journal.

\* Corresponding author.

E-mail address: [aorjuelal@unal.edu.co](mailto:aorjuelal@unal.edu.co) (A. Orjuela).

<https://doi.org/10.1016/j.cej.2025.159907>

Available online 27 January 2025

1385-8947/© 2025 The Author(s). Published by Elsevier B.V. This is an open access article under the CC BY-NC-ND license (<http://creativecommons.org/licenses/by-nc-nd/4.0/>).

chains. Despite the observed variability, over 90 % of UCOs consist of triglycerides with diverse fatty acid chains and variable degrees of unsaturation [5,11]. This characteristic is particularly relevant for producing epoxidized oils, as the epoxy or oxirane groups (cyclic ethers) are generated in olefinic bonds of the fatty acid chains. Epoxidized vegetable oils are value-added oleochemical derivatives that are currently used as plasticizers and stabilizing agents in plastic products as well as intermediates in the manufacturing of polymers and resins [12,13,14]. Therefore, using UCOs would aid in the transition to greener materials for the polymer industry and promote sustainability in the oleochemical sector.

Epoxidation reaction can be carried out through various chemical pathways using different oxidizing agents, including percarboxylic acids, organic and inorganic peroxides, haloalcohols, ozone, and even molecular oxygen [15,16,17]. In general, the process can be carried out by means of conventional homogeneous catalysis, but also with heterogeneous ones (e.g., using ion exchange resins) [18], by chemoenzymatic epoxidation [19,20], in the presence of polyoxometalates [21,22] and using phase-transfer catalysts [23,24,25]. The conventional method is generally employed at the industrial scale, and it is conducted via the Prileschajew reaction (Fig. 1) between an unsaturated oil and  $H_2O_2$ , using a percarboxylic acid generated in situ as an oxygen carrier and  $H_2SO_4$  as catalyst [26,27,28]. This reaction occurs in a two-phase system that requires high shear mixing to ensure effective mass transfer of the oxygen carrier between the aqueous and oil phases. However, this also promotes emulsion formation, hindering downstream separation through decanting. Additionally, the reaction is highly exothermic, and the oxirane groups can be prone to thermally-driven, acid-catalyzed ring-opening reactions with different components of the reactive medium. While the conventional approach allows for high reaction rates and conversions, the process encounters challenges such as complex temperature control, low selectivity, and the generation of undesirable byproducts such as glycols, hydroxyesters, ketones, and polyols, among others [26].

Since some of the challenges of the conventional process stem from the mass and heat transfer limitations, process intensification (PI) could significantly enhance epoxidation reactions. In particular, implementing advanced reactor designs and process automation would help improve reaction efficiency, product quality and facilitate downstream separation [29,30]. PI has become critical in the chemical industry, aiming to optimize reactions through more efficient technologies. By integrating operations, functions, and phenomena or by enhancing specific phenomena in an operation, unit, or process, the PI approach leads to substantially smaller, cleaner, and more energy-efficient technologies [31,32,33]. In the particular case of liquid–liquid epoxidation reactions, and considering the clustering of PI approaches in the four domains [33], the spatial domain can be exploited by using segmented flow milli- or micro-reactors, also known as slug-flow reactors [34,35,36]. In these

continuous operating devices, alternating slugs of the two-phase reaction mixture allow for exceptionally high convective transport within the slugs and significantly enhanced diffusion rates between adjacent slugs. Intensification of mass transfer occurs by the turbulent internal circulation caused by the shear between continuous phase/wall surface and slugs, thus boosting diffusive penetration and, consequently, the reaction rates [37]. Moreover, the high ratio of heat transfer area to reactor volume in millireactors and the high volumetric heat removal capacity allow for better temperature control in exothermic reactions and the mitigation of thermally-driven side reactions. This characteristic can also be leveraged in industrial scale-up through a numbering-up strategy, such as employing a shell-and-tube heat exchanger and reactor configuration [38,39,40,41]. Additionally, as the high mixing is achieved without turbulent dispersion, downstream separation of immiscible phases can be readily accomplished by decantation.

This work aimed to develop a semi-automatic platform for the continuous epoxidation of UCOs using slug-flow millireactors. The platform was designed to optimize various operational conditions, maximizing conversion, selectivity, and productivity while minimizing the risk of phase coalescence that could disrupt the slug-flow regime. Through careful control and monitoring of reactor conditions via the semi-automated system, the main goal was to demonstrate a scalable, reproducible, efficient, and safe process for the valorization of UCOs. To identify a suitable operating window, the study includes a detailed analysis of the effects of various operating parameters on the epoxidation process, such as phase ratios, residence time, and temperature. Additionally, we explore the impact of coalescence on the overall process efficiency during the epoxidation of UCOs and other virgin vegetable oils. This work aims to provide valuable insights into optimizing UCOs epoxidation in slug-flow millireactors for further scale up and potential industrial deployment by presenting a comprehensive overview of the obtained results.

## 2. Materials and Methods

### 2.1. Reagents and chemicals

Hydrogen peroxide ( $H_2O_2$ , 50 wt%, Carl Roth GmbH + Co. KG), sulfuric acid ( $H_2SO_4$ , 99.5 wt%, Carl Roth GmbH + Co. KG), and acetic acid ( $AcOH$ , 100 % v/v, Sigma-Aldrich) were utilized as reagents for the epoxidation reaction. Deuterated chloroform ( $CDCl_3$ , 99 Atom% D., Carl Roth GmbH + Co. KG) served as the solvent for monitoring the reaction via  $^1H$  NMR. Additionally, various commercial oils were employed for comparative analysis, including soybean oil (Carl Roth GmbH + Co. KG), linseed oil (Carl Roth GmbH + Co. KG), sunflower oil (Brökelmann + Co. – Ölmühle GmbH + Co.), and canola oil (Brökelmann + Co. – Ölmühle GmbH + Co.). Karl Fisher analysis used a coulomat oil solution (Hydranal()) for water determination.

The used cooking oil (UCO) was obtained from two sources: the first was a blend of UCOs collected in chicken restaurants in Bogotá-Colombia, and the second was obtained from a household in Germany. The origin of the first batch was selected considering previous reports [42] indicating that, despite the challenges posed by its deteriorated physicochemical properties, UCOs from chicken restaurants might have high iodine value (119 – 72 g  $I_2/100$  g of oil). The second batch was collected to provide a more favorable scenario for evaluating the epoxidation platform. Subsequently, mixtures were prepared between both UCOs to determine the specifications that ensure stable operation. Both batches of collected UCO were separately homogenized by stirring at 500 RPM and heated to over 60 °C to facilitate filtration. Subsequently, the oils were vacuum filtered using 90 mm diameter 12–25  $\mu m$  filter paper (Macherey-Nagel) to remove suspended solid particles. Finally, the oils were stored in amber glass bottles at room temperature before use.

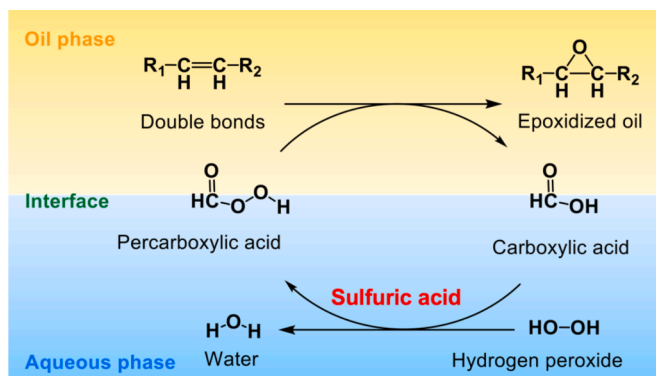


Fig. 1. Scheme of two-phase epoxidation via Prileschajew reaction using an acid catalyst.

## 2.2. Characterization of samples

The monitoring of the epoxidation reaction and the characterization of the different feedstock materials (i.e., UCOs and vegetable oils) were performed through the measurement of iodine value (IV) and oxirane value (OV) using  $^1\text{H}$  NMR spectroscopy, following the methodology described in previous work [34], and based on Equation (1) and Equation (2), respectively.

$$IV = \left( 26.039 \cdot \frac{2 \cdot A_{DB}}{A_{ref}} \right) - 5.7358 \quad (1)$$

$$OV = \left( 1.4446 \cdot \frac{2 \cdot A_{OR}}{A_{ref}} \right) + 0.4643 \quad (2)$$

Here,  $A_{DB}$  is the area below the signal between 5.36 – 5.65 ppm corresponding to the double bonds,  $A_{ref}$  is the area produced by the characteristic peak of the reference group (i.e. glyceryl),  $A_{OR}$  is the area below the peak of the chemical shift between 2.85 – 3.22 ppm corresponding to oxirane oxygen. The preparation and measurement of the samples were conducted on the same day to minimize the possibility of oxirane ring degradation.

The dynamic viscosity of oils was also measured at different temperatures to identify differences in fluidity within the reactor using a shear rheometer (MCR302, Anton Paar, Ostfildern-Scharnhausen, Germany). The measurements were performed with cone-plate geometry, using a diameter of 12 mm (CP-12, 0.025 mm gap,  $1^\circ$  cone angle; Anton Paar, Ostfildern-Scharnhausen, Germany). Humidity content in samples was measured by Karl Fisher titration using a 756 KF Coulometer (Metrohn), and the content of polar compounds was measured by a capacitive method using a Testo® 270 portable meter. The apparatus was previously calibrated using a reference oil of 2.5 % total polar compounds.

## 2.3. Epoxidation platform

The epoxidation platform schematically depicted in Fig. 2 was built as a semi-automated system for startup, continuous operation, periodic sampling, and real-time process control. The employed configuration was based on a detailed study that previously explored the effect of reactor design, mixing points, and required accessories [34]. The system integrated three dosing syringe pumps (Harvard Apparatus Pump 11 Elite) that allowed the fine-tuning control of flow rates of the input

streams: oil,  $\text{H}_2\text{O}_2$ , and acids ( $\text{H}_2\text{SO}_4$  and acetic acid). This control granted the slug-flow pattern under different operating conditions. The millireactor corresponded to a perfluoroalkoxy alkane (PFA) tubing with an internal diameter of 1.62 mm, an external diameter of 3.18 mm, and a length of 2.62 m, establishing a reaction volume of 5.37 mL. It was submerged in a glass container connected to a thermostatic water recirculation bath (Huber Model CC508) to maintain strict temperature control ( $\pm 0.1^\circ\text{C}$ ). The temperature monitoring of the slug-flow reactor was carried out via a thermocouple connected to the interior of the reactor outlet. Additionally, the oil feed stream was heated using an electric heating wrap (Svbonny Model SV172), which maintained the temperature above  $60^\circ\text{C}$  to ensure the fluidity of UCO (syringe pump 1, Fig. 2). Furthermore, the system included a multiposition valve (Knauer Valve Drive V 2.1S) to collect up to 16 samples during continuous operation. The microsyringe pumps provided precise volumetric flow control at variable peak pressures ( $< 7$  bar). Although the operating pressure was not directly measured, it was anticipated to be low due to the reactor outlet being at atmospheric pressure, the incompressibility of both fluids and the very low flow velocities. Consequently, the system was expected to operate under low pressure with minimal pressure drop.

The epoxidation was accomplished by reacting the oil and  $\text{H}_2\text{O}_2$ , using peracetic acid generated in situ as the oxygen carrier and  $\text{H}_2\text{SO}_4$  as the catalyst. Initially, glass syringes were fully loaded with raw materials: UCO or vegetable oil,  $\text{H}_2\text{O}_2$ , and an acid solution. The acid solution was pre-weighed and consisted of 71.09 wt% acetic acid and 28.91 wt%  $\text{H}_2\text{SO}_4$ . These concentrations were the most efficient from a previous study promoting epoxidation without triggering oxirane ring-opening reactions [34]. In that study, the composition was thoroughly assessed on the experimental platform during the epoxidation of soybean oil. It was found that increasing the  $\text{H}_2\text{SO}_4$  concentration led to a reduction in acetic acid, which negatively impacted both conversion and selectivity. The excess catalyst facilitated unwanted ring-opening reactions, while the lower acetic acid content hindered peracetic acid formation, a crucial oxygen carrier for epoxidation. Conversely, a high acetic acid content combined with a low  $\text{H}_2\text{SO}_4$  concentration resulted in poor conversions and selectivities due to inadequate peracetic acid production. The UCO employed was also maintained under stirring at  $60^\circ\text{C}$  before being loaded into the syringe.

Automation of the platform was implemented using Flowchem python package, which allowed controlling laboratory instruments and devices through Python programming script [43]. Three syringe pumps, a thermostatic bath, and a multiposition valve were connected via

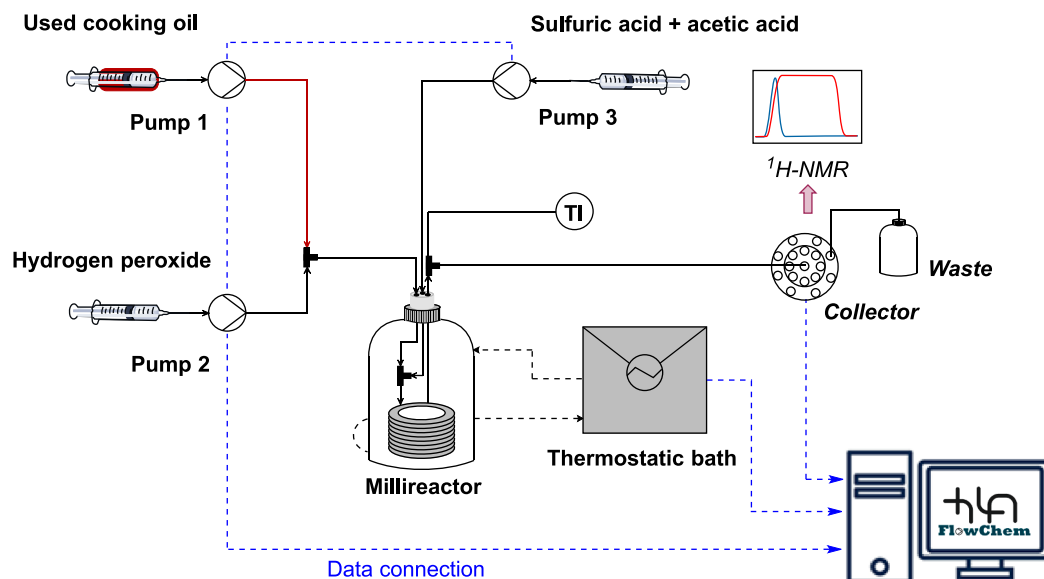


Fig. 2. Experimental setup of the slug-flow reactor used in epoxidation reaction. (—) Tubing connection, (---) Insulated tubing connection and (---) Data connection.

Flowchem, a computer, and a custom code in Python was developed to carry out the system operation. The script consisted of various functions and processes, detailed in the flowchart of Fig. S1 in the supplementary material. The user manually entered the input variables, and they included the experiment code, the number of samples to be collected, and the operational conditions such as residence time, the ratio of H<sub>2</sub>O<sub>2</sub> to oil, the ratio of acid to oil, and temperature. Based on these inputs, the software automatically calculated the required initial and operating flow rates of the inlet streams. The initial flow rates were set to double the calculated operating flow rates to expedite the filling process, ensuring rapid temperature stabilization while maintaining the same phase proportions. Subsequently, the operating parameters of the equipment were configured, initiating the reactor filling and heating until the target temperature was reached. Once the system stabilized, the reaction parameters (oil flow rate, H<sub>2</sub>O<sub>2</sub> flow rate, acid flow rate, and temperature) were established, and the continuous operation of the reaction was initiated. Sample collection started after operating 1.6 times the configured residence time, ensuring that a representative sample of the system at steady state was obtained. 2 mL samples were collected along the epoxidation reaction, and the stability of the system was verified to ensure the reproducibility of the data.

#### 2.4. Process optimization

Operating conditions were optimized during UCO epoxidation using a simplex evolutionary operation. This method allows for the simultaneous manipulation of multiple variables and constraints in the system, thus optimizing the selected response variables. The simplex evolutionary operation method, schematically described in Fig. S2 in the supplementary material, involves generating an initial matrix that contains different experiments or vertices at specific operating conditions, enabling efficient navigation through a defined solution space. A new potential vertex is proposed (i.e., a new set of operating conditions), generating a new matrix with each iteration, bringing the system closer to an optimum [44].

The variables selected for optimizing the epoxidation process were: i) the ratio between flow rates of H<sub>2</sub>O<sub>2</sub> and oil, ii) the ratio between flow rates of acids and oil, iii) residence time, and iv) reaction temperature. Drawing from prior evaluations of the platform performance [34], the chosen optimization variable was productivity, as it allows for an appropriate comparison with other types of continuous and batch reactors. However, selectivity, conversion, and final oxirane value were also considered for analysis and decision-making to meet product specifications. The step sizes and initial values for the experimental optimization are reported in Table S.1 of the supplementary material, and they were based on the optimal conditions previously identified for soybean oil on the platform.

This chart was constructed from a correlation matrix that established the relationships between the independent variables (temperature, H<sub>2</sub>O<sub>2</sub>/oil ratio, acid/oil ratio, and residence time) and the target response variables (productivity, selectivity, conversion, yield, and oxirane value). The Pareto chart ranked these correlations based on their relative impact on the target variables, enabling the identification of the most influential factors. This approach provided an efficient tool for quantitatively interpreting the observed effects and prioritizing key parameters in the intensification of the epoxidation process.

#### 2.5. Response variable definition

The selected response variable for optimization was productivity (P), which was determined using Equation (3), involving the feed oil flow rate (mL/min), as well as the conversion (X) and selectivity (S) of the reaction system. Equations (4), 5, and 6 define the conversion, selectivity, and yield. In this context, IV refers to the iodine value of the oil before the reaction (denoted by sub-index 0) and after the reaction (denoted by sub-index i).

$$P = \frac{X \cdot S \cdot \text{Flow}_{\text{oil}}}{V_{\text{reactor}}} \cdot \frac{IV_0 \cdot \rho_{\text{oil}} \cdot MW_0}{MW_{I_2} \cdot 100000} \quad (3)$$

$$X = \frac{(IV_0 - IV_i)}{IV_0} \quad (4)$$

$$S = \frac{\frac{OV_i}{16}}{\frac{(IV_0 - IV_i)}{253.8}} \quad (5)$$

$$Y = X \cdot S \quad (6)$$

In the equation,  $V_{\text{reactor}}$  represents the reactor volume, which is 5.37 cm<sup>3</sup>,  $\rho_{\text{oil}}$  denotes the density of the oil (920 kg/m<sup>3</sup>),  $MW_{I_2}$  is the molecular weight of iodine (I<sub>2</sub>), which is 253.81 g/mol and. and  $MW_0$  is the molecular weight of oxygen, which is 16 g/mol.

### 3. Results and discussion

#### 3.1. Characterization of UCOs

Heterogeneity is an intrinsic characteristic of UCOs due to multiple impurities, the different types of vegetable oils used in cooking practices, and the conditions during use (e.g., cooking temperature, use time, processed food, cooking ware materials, etc.) and handling. Table 1 compares the physicochemical properties of the UCOs used in this study and previously reported results for oils from similar sources.

The properties of assessed UCOs are generally in the same range of samples previously collected in different restaurants in Bogotá, Colombia [45,42]. The quality of UCOs is commonly evaluated indirectly through the measurement of the saponification index and the acid value [46,47]. The saponification value is a fundamental property that provides insight into the composition of UCOs and allows for an estimation of the average molecular weight of constituent triglycerides. In this case, the saponification value and corresponding average molecular weight in the collected sample from Bogotá-Colombia (i.e. First batch) are consistent with a high palm oil content. In the hosteling sector of the city, it is common to use blends of vegetable oils to maintain a liquid product at ambient conditions (6–20 °C), but at a lower cost and with a high stability for extended reuse. This is also confirmed by the low IV of the samples, which is similar to that of high oleic palm oil or of mixtures of unsaturated oils with traditional palm oil [48,49]. The second batch of UCO exhibited a high iodine value, similar to that observed in sunflower or canola oil, which are highly consumed in Germany for food preparation. The acidity content indicates the degree of hydrolysis, which provides insights regarding proper use and storage. The high acid value is common in highly reused cooking oils and in UCOs that are improperly stored (i.e., with water in the containers). The acid value in the sample from Colombian restaurants was higher than the allowed for edible oils (0.6 mgKOH/g.; [50]), but this was expected due to extended

**Table 1**  
Physicochemical properties of collected UCOs and comparison with previous reports.

Properties	[42]	[53]	First batch	Second batch
Saponification value, mg KOH/g	205.54 – 178.44	206.17 ± 0.92	186.55	192.04
Average molecular weight, g/mol	822.51 – 1041.83	829.93	992.73	877.34
Acid value, mg KOH/g	16.88 – 0.9	3.36 ± 0.12	17.0	0.19
Iodine value, gI <sub>2</sub> /100 g	119.01 – 72.29	88.68 ± 0.01	79.10 ± 1.07	117.95 ± 0.09
Total polar compounds, %	40.0 – 14.2	> 40.0	35.0	2.0
Humidity, wt.%	–	1.344	0.527	0.004

reuse and moisture in the samples. The presence of unsaturated free fatty acids might affect the quality of epoxidized UCO due to the formation of low molecular weight epoxides, and the remnants of saturated fatty acids would affect the plasticizing performance. Also, free fatty acids increase the polarity of the oil phase, which is of significant concern for the operation of the slug flow reactor.

Polar compound content describes the degree of oil degradation, as it identifies substances such as free fatty acids, monoglycerides, diglycerides, and oxidation products like aldehydes and ketones. These are generated from the degradation reactions (i.e., oxidation, hydrolysis and polymerization) that the oil undergoes during frying[51]. Also, the high content of polar compounds could impose hydrodynamic challenges in the slug flow, as their polarity might increase the chances of emulsification, phase coalescence, and water uptake in the oil phase. Additionally, a high content of polar compounds hinders the downstream separation of reactor effluents, which is critical to the efficiency of the process. In contrast, the household UCO collected in Germany exhibited less degradation with a low content of polar compounds, making it less problematic for further use.

### 3.2. The iodine value of vegetable oils and UCOs

Commercial vegetable oils were characterized using  $^1\text{H}$  NMR; as shown in Table 2, all exhibited a high iodine value. This is essential to ensure that epoxides meet the requirement of a high content of oxirane oxygen, both for industrial-grade applications ( $\geq 3.5$  wt%) and for food and pharmaceutical-grade applications ( $\geq 6.0$  wt%). Generally, an IV  $\geq 70$  g  $\text{I}_2/100$  g is required to meet the specifications of industrial-grade epoxidized oils, which is the target market for epoxidized UCOs. Since epoxidized UCOs may still contain impurities of uncertain nature, it is essential to avoid direct contact with humans and animals to minimize health risks. The corresponding maximum theoretical OV were all above  $\geq 3.5$  wt%, confirming that the evaluated oils were suitable feedstocks for further epoxidation.

### 3.3. Viscosity of UCOs

A suitable viscosity of fluids is crucial for maintaining proper hydrodynamic patterns in the slug-flow reactor, so it was characterized for the collected UCO, the refined vegetable oils, and a sample of commercial epoxidized oil. This was required due to the challenges of maintaining a continuous fluid flow through the tubing and creating alternating slugs at the inlet mixing point. Since viscosity can significantly affect interaction and coalescence between oil and aqueous phases within the reactor, more operating challenges were expected during UCO epoxidation. This was confirmed by the observation in Table 3 that the viscosity of UCOs at low temperatures was higher than that of vegetable oil and comparable to that of epoxidized vegetable oil. In UCOs, impurities from degradation and polymerization reactions and a higher content of saturated fatty acid chains in triglycerides result in increased viscosity and challenges with fluidization and transport processes. The UCO sourced in Colombia showed a higher viscosity at low temperatures, reflecting its greater palm oil content. This accounted for the flow issues observed on the platform, particularly the clogging of the

**Table 2**

The iodine value of tested vegetable oils and UCOs and maximum theoretical oxirane value.

Raw material	Iodine value, g $\text{I}_2/100$ g oil	Maximum theoretical oxirane value, wt%
Linseed oil	172.59	10.9
Soybean oil	130.97	8.3
Sunflower oil	124.46	7.8
Canola oil	111.44	7.0
UCO First batch	79.10	5.0
UCO Second batch	117.95	7.4

**Table 3**

Dynamic viscosity of UCOs, soybean oil, and epoxidized soybean oil.

Temperature, °C	Viscosity, cP			
	Soybean oil	Epoxidized soybean oil	UCO First batch	UCO Second batch
25	51.51	63.37	89.49	59.04
60	19.13	18.84	19.04	18.71
70	8.29	15.46	15.17	15.46

feed pump. Nonetheless, the viscosity of all samples decreased above 60 °C. Then, in subsequent experiments, a heating wrap system was installed around the syringe and in the UCO feed line, maintaining temperatures at 60 °C before entering the reactor. This adjustment significantly reduced the viscosity of UCOs and improved fluidity in the tubing and the formation of the slug-flow patterns.

### 3.4. Evaluation of platform compatibility with UCOs and commercial oils

The epoxidation platform was preliminarily evaluated with UCOs and different commercial vegetable oils selected for their common use as epoxidation feedstocks. Assessing diverse raw materials in the epoxidation platform allows for determining the versatility and reliability of the system in handling highly heterogeneous raw materials. In the case of UCOs and other waste fats and oils that contain significant impurities and that are often mixtures of various vegetable oils, this evaluation is essential for establishing the robustness of the system. The different oils were evaluated on the platform under the same operating conditions previously obtained from an optimization study using soybean oil[34]. The evaluated conditions included an oil flow rate of 0.087 mL/min, a volumetric flow ratio of  $\text{H}_2\text{O}_2$  to oil of 0.79:1, a volumetric flow ratio of acids to oil of 0.29:1, a residence time of 29.56 min, and a reaction temperature of 68.9 °C. The corresponding results of conversion, selectivity, and yield are presented in Fig. 3.

As observe, similar behaviors were obtained for all commercial vegetable oils, showing high conversions (87 %), selectivities (85 %), and yields (79 %), with the exception of linseed oil. In this case, despite the higher IV that indicated greater availability of double bonds for epoxidation, the main drawback was the low viscosity (2–8 cP). This oil did not facilitate the adequate hydrodynamic performance of the slug-flow reactor under the assessed conditions, limiting the utilization of its high unsaturation content. However, it is anticipated that under specific operating conditions, significantly improved performance could also be obtained with linseed oil. While it was not further investigated as it fell outside the scope of this study, this highlights the significant impact of oil viscosity on the proper performance of the slug-flow epoxidation reactor. Regarding the performance with UCOs, using the sample collected in Colombia (i.e. first batch) resulted in low conversion and yield, as it was impossible to achieve proper slug flow patterns in the reactor due to high coalescence between the phases. This was attributed to the strong affinity of the oil for the aqueous phase due to the larger content of polar compounds that triggered the emulsification of the immiscible phases. In contrast, operating with the UCO collected from a household in Germany (i.e., second batch), it was possible to obtain good results in conversion, selectivity, and yield, closely approaching those obtained with the refined vegetable oils. This was expected given the higher IV and its optimal performance in the reactor, where no phase coalescence was observed.

In addition to the above, special attention must be given to the OV, as it ensures compliance with the product specifications and influences its market price. The oxirane oxygen content of the obtained epoxides at the reactor outlet stream are presented in Fig. 4. It can be noticed that all oils met the minimum specifications of industrial-grade epoxidized oil ( $>3.5$  wt%), except for the UCO from the first batch, which had an oxirane index of 2.70 wt%. This was expected due to its poor performance in the epoxidation and the inadequate hydrodynamic behavior in

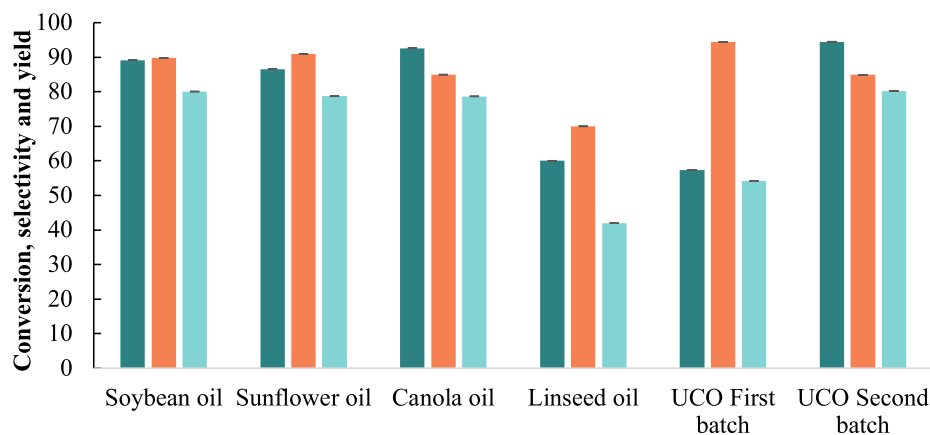


Fig. 3. Conversion (■), Selectivity (■) and Yield (■) results of different vegetable oils and UCOs under the same operating conditions in the epoxidation platform.

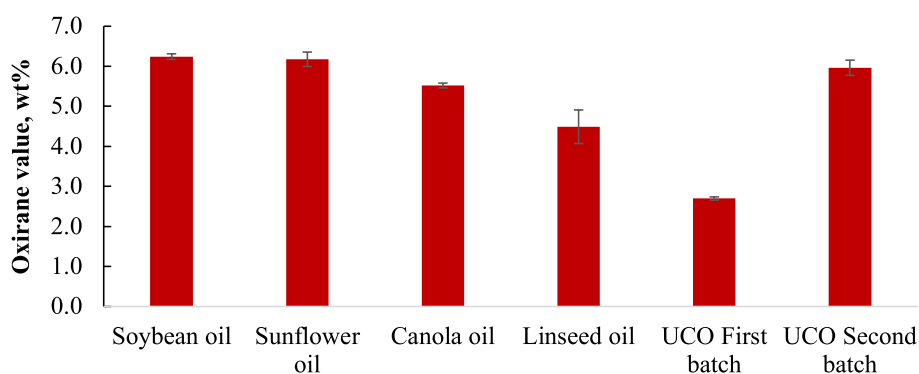


Fig. 4. Final oxirane value results of different vegetable oils and UCOs under the same operating conditions in the epoxidation platform.

the slug-flow reactor. Comparatively, soybean and sunflower oils reached oxirane index values exceeding 6.0 wt%, thus meeting the specifications for food-grade and pharmaceutical-grade epoxidized oil.

### 3.5. Exploratory assessment with UCOs

Considering the preliminary results with the assessed UCOs, different blends of the collected batches in Colombia and Germany were prepared to determine the minimum specifications required for a suitable performance in the studied epoxidation platform. On the one hand, there is a need to ensure that the IV of the feedstock is high enough to achieve the minimum OV required for industrial-grade epoxidized oil. Furthermore, it is essential to ensure the proper fluidity of the oil to achieve the required slug flow patterns and high mass and heat transfer rates within the system. In this regard, mixtures of different proportions of UCOs from the first and second batches were prepared. The mixtures were homogenized at 60 °C, characterized using  $^1\text{H}$  NMR to verify the resulting IV (see Table 4), and evaluated in the epoxidation platform.

Fig. 5 summarizes the conversion and selectivity obtained under the IV increased with the higher proportion of UCO from the second batch. The increase in conversion employing a blend feedstock was mainly due to the reduction in coalescence between the phases. As the UCO from the second batch had a lower affinity for the aqueous phase, a better slug flow pattern was achieved, and the reactor performed better. This was confirmed by visual inspection of the reactor slug pattern. Blends containing over 20 % wt of higher quality UCO enabled a steady slug flow operation without phase coalescence. It was noticed that beyond this content, the conversion stabilized and no further dilution was necessary to obtain suitable epoxidation.

A mixture containing 30 % UCO from the second batch was used for further evaluation in the reactor, assuring hydrodynamic stability. The

Table 4  
Iodine value of the UCO mixtures from the first and second batch.

Proportion, wt% UCO First batch	UCO Second batch	Iodine value, g I <sub>2</sub> /100 g oil		Humidity, wt%
		Theoretical	Experimental ( $^1\text{H}$ NMR)	
100.0	0.0	79.10	79.10	0.527 ± 0.07
90.0	10.0	82.99	83.40	0.381 ± 0.04
79.9	20.1	86.89	86.40	0.308 ± 0.04
74.0	26.0	88.81	87.40	0.296 ± 0.03
70.0	30.0	90.75	90.67	0.234 ± 0.04
60.1	39.9	94.61	94.41	0.237 ± 0.05
49.8	50.2	98.55	97.34	0.170 ± 0.02
0.0	100.0	117.95	117.95	0.004 ± 0.01

corresponding properties of the mix were: Saponification value of 192.84 mg KOH/g, acidity of 8.26 mg KOH/g, IV of  $90.67 \pm 1.57$  gI<sub>2</sub>/100 g oil, a total polar compounds content of 17.0 % and a humidity of 0.234 %. According to the preliminary results of Fig. 5, this blend enabled to achieve an epoxide value of 3.56 wt%, fulfilling the specifications of industrial-grade epoxidized oil. It is important to note that while a decrease in viscosity was anticipated when using the mixture of UCOs, the impact of this change was assumed to be minimal. Then, the preheating system in the feed line was maintained to ensure that the viscosity of UCO was low enough to facilitate proper fluidity in the

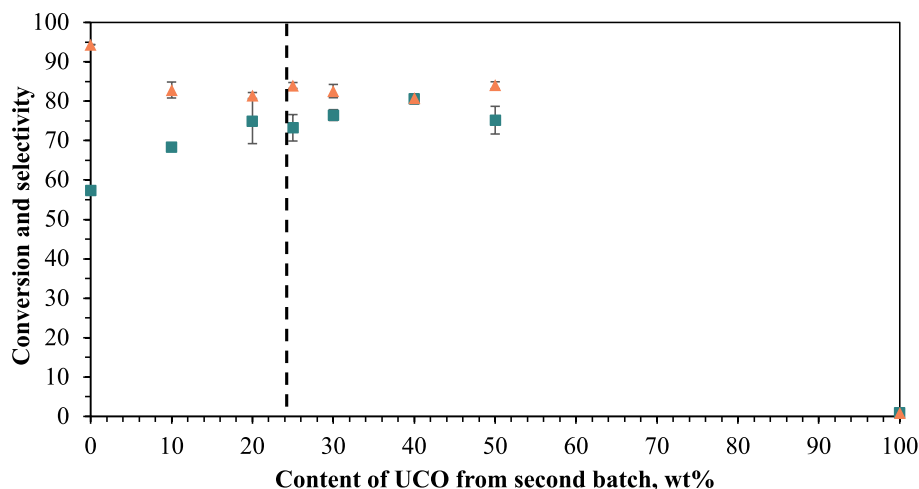


**Fig. 5.** Conversion (■) and Selectivity (▲) results were obtained during the epoxidation of mixtures of UCOS prepared with samples collected in the hosteling sector in Colombia (first batch) and households in Germany (Second batch). Operating conditions in the epoxidation platform: oil flow rate of 0.087 mL/min, a volumetric flow ratio of H<sub>2</sub>O<sub>2</sub> to oil of 0.79:1, a volumetric flow ratio of acids to oil of 0.29:1, residence time 29.56 min, and temperature of 68.9 °C.

reactor.

As previously mentioned, generating a stable slug-flow regime in the reactor is essential to promote effective mass and heat transfer between the phases. However, the UCO from the first batch failed to create a regular flow due to a high affinity for the aqueous phase, consistent with the higher humidity and content of polar compounds reported in Table 4. This affinity triggered significant coalescence in the flow, forming large phase blocks or causing irregular flow through the tubing. Then, oil water content and the concentration of polar compounds could serve as valuable indicators to determine if a UCO would be suitable for epoxidation in the proposed reactor. According to the results, the processed UCOS should have maximum moisture lower than 0.234 wt% and a total polar components content below 17.0 % to ensure proper behavior in the slug-flow reactor system. These parameters are crucial in influencing the hydrodynamics and efficiency of the segmented flow. Elevated levels of polar compounds can disrupt the interfacial tension between immiscible phases, impairing slug formation and stability. Similarly, high moisture levels may promote undesirable side reactions, such as oxirane ring opening during epoxidation, reducing process selectivity. Furthermore, these parameters can serve as surrogates to determine the necessity of pretreatment before millireactor processing and identify the most suitable processing strategies.

Some oil pretreatment can be employed, such as decanting for water removal, filtration to remove solid particles, degumming to eliminate phospholipids and polar compounds, and solvent extraction for the efficient removal of polar compounds and free fatty acids [52,5,45,53]. For instance, 77 % of free fatty acids and 53 % of total polar compounds have been removed utilizing solvent extraction [52,45]. These operations improve the physicochemical properties of the oil, ensuring consistent and reliable performance in the slug-flow reactor for this type of feedstock.

### 3.6. Effect of volumetric flow ratio between aqueous and oil phases

Besides the intrinsic characteristics of UCOS, the ratio of flow rates between the aqueous and oil phases is a crucial variable to ensure the slug-flow regime. Improper selection of this ratio could trigger phase coalescence or segmented flow, which reduces the mass transfer area and, consequently, reaction performance. In a previous study on the epoxidation of soybean oil in the slug-flow millireactor, the suitable operating ratio ranged from 0.94 to 2.50. However, from the preliminary tests, coalescence was observed when operating under these conditions. This confirms that there are specific operating ranges to

ensure optimal performance for each specific oil. This outcome was somewhat anticipated, given the poor performance observed in the epoxidation of linseed oil, which has one of the highest IV among commercial oils despite being commonly used in producing epoxidized vegetable oil plasticizers. Then, it was necessary to determine a range of aqueous-to-UCO flow ratios to ensure a proper slug-flow regime. In these experiments, the volumetric flow rates of each phase were set to maintain a constant residence time of 29.56 min., with a fixed proportion between acid and H<sub>2</sub>O<sub>2</sub> flow rates in the aqueous phase. The slug-flow regime was visually inspected for each ratio to verify the absence of phase coalescence or segmentation. Fig. 6 summarizes the conversion, selectivity, and productivity results of the different volumetric ratios.

While conversion increased with higher loading of the aqueous phase, selectivity towards oxirane groups decreased within the evaluated operating range (right section on Fig. 6). The acid proportion in the system increases with the aqueous phase, which promotes ring-opening reactions. Similarly, conversion was significantly affected by the phase ratio. Below a volumetric ratio of 1.08, significant coalescence was observed in the oil phase with a subsequent decrease in conversion (see Fig. S1 in the supplementary material). Besides a lesser amount of acid solution, the coalescence reduces the mass transfer of the oxygen carrier and the effectiveness of the reactor. Above a volumetric ratio of 1.08, a slight increase in conversion was observed, and no coalescence was visually detected in the reactor up to a ratio of 2.0. This suggests that this increase in conversion is primarily associated with the rise in the aqueous phase rather than with issues related to coalescence in the slug-flow regime. However, coalescence was again evidenced when the ratio exceeded 2.0, but this time in the aqueous phase (see Fig. S3 in the supplementary material). Although it was still possible to maintain a high and constant conversion even as the ratio increased, the selectivity dropped, and so did the productivity of the reactor (i.e., lower oil flow rates). Again, high loadings of the oxidant agent triggered ring-opening reactions, and low oil flow rates reduced reactor productivity. It is important to note that greater fluctuations in results were observed when there was coalescence between phases, leading to higher error margins since conditions were neither stable nor reproducible in the system. Consequently, it was experimentally verified that a proper operation could be conducted using a phase ratio between 1.08 and 2.0.

### 3.7. Optimization

Based on the exploratory tests with UCOS and verifying that process performance was influenced solely by reaction performance and not by

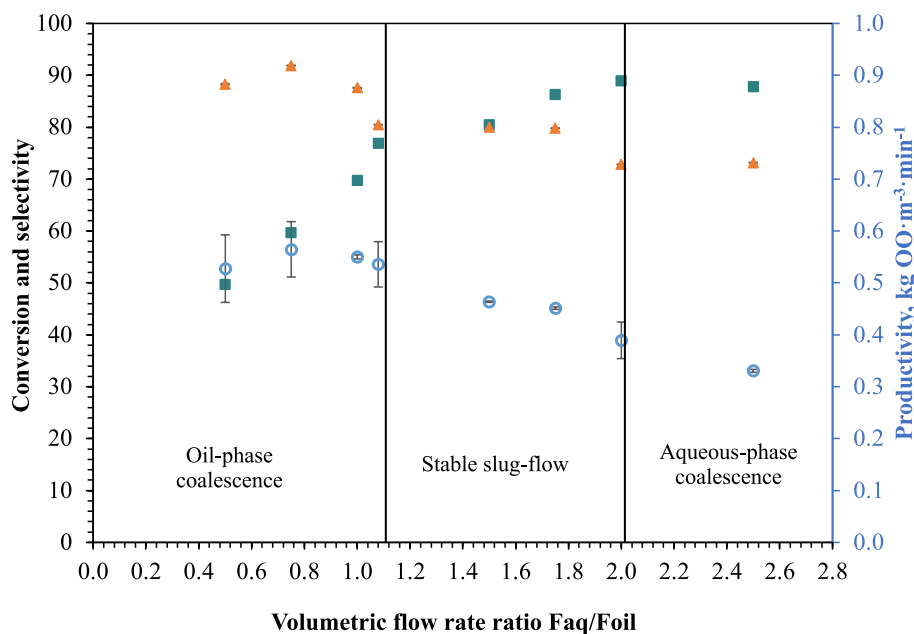


**Fig. 6.** Conversion (■), Selectivity (▲), and Productivity (○) results in the epoxidation platform operating with different proportions of aqueous phase to UCO. Operation conditions: oil flow rate of 0.087 mL/min, volumetric flow ratio of H<sub>2</sub>O<sub>2</sub> to oil of 0.79:1, volumetric flow ratio of acids to oil of 0.29:1, residence time of 29.56 min, and temperature of 68.9 °C.

hydrodynamic limitations of the system (i.e., coalescence), it was possible to optimize the performance of the epoxidation platform. The assessed variables during experiments were temperature, residence time, the volumetric flow ratio of H<sub>2</sub>O<sub>2</sub> to oil, and the ratio of acid to oil. The last two variables are also described in the results as the volumetric flow ratios of the aqueous to the oil phase. Fig. 7 illustrates the exploratory space during optimization using the simplex evolutionary operation method, in which 17 experiments were conducted. In the supplementary material are reported the initial conditions of the optimization process (Table S2), those during the evolution of the simplex (Table S3), the corresponding Reynolds numbers of the aqueous slugs and oil phase [54,40] and the obtained results along the process

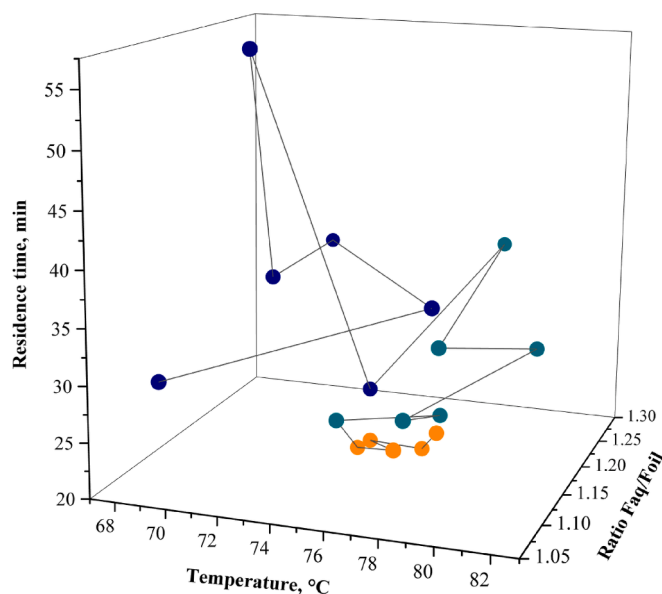


**Fig. 7.** Evolution of the exploratory space during optimization of the slug flow reactor in the epoxidation of UCO (●) Initial points of the simplex algorithm. (●) Points of evolution to the optimal conditions. (●) Points near the optimal operation.

(Fig. S4).

It can be observed that the initial points explored a wide range of experimental conditions, but as the optimization algorithm progressed, it entered in an iterative phase where it gradually converged towards an optimal region, represented by the vertices in green and orange. The final vertices (orange dots) corresponded to the final set of experiments where no statistically significant differences in productivity were observed, indicating that the optimal solution was reached. The orange vertices tend to cluster in regions at higher temperatures and lower residence times, suggesting that a trade-off between reaction kinetics of competing reactions achieved favorable conditions. At higher temperatures, the reaction rates of epoxidation increased together with the mass transfer rates of the oxygen carrier between phases, but reducing residence time limited the progression of the ring-opening reactions. The separate results of conversion, selectivity, productivity and oxirane oxygen content along the optimization process are presented in Fig. 8. The yield results are presented in Fig. S5 in the supplementary material. The three-dimensional diagrams allow for analyzing the effects of residence time, temperature, and the volumetric flow ratio of the aqueous and oil phases, with all response variables represented on a color scale.

Fig. 8a illustrates the impact of the conversion of double bonds in UCOs. The lowest conversions were  $X = 0.58$  for experiment 5 and  $X = 0.73$  for Experiments 1 and 3, corresponding to the initial exploratory experiments. As the iterations evolved, conversion values increased above 0.81, indicating that evaluated variables positively influenced this response variable. As expected, the highest conversions were predominantly observed at elevated temperatures ( $\sim 78$  °C) but, surprisingly, under shorter residence times ( $\sim 25$ – $30$  min.). While high temperatures have a major impact on the rates of reaction and mass transfer coefficients, it was expected that shorter residence times might hurt the process effectiveness. However, it is essential to consider the hydrodynamic behavior of the reactor and the high impact of internal circulation within the slugs to ensure effective diffusive penetration and high mass and heat transfer rates. At high residence times, the reactive flow rate was reduced (i.e., 39% from 0.2423 to 0.0937 mL/min), so the velocity of the slugs. This reduces the internal circulation and the turbulence between continuous phase/wall surface and slugs, as well as between adjacent slugs.



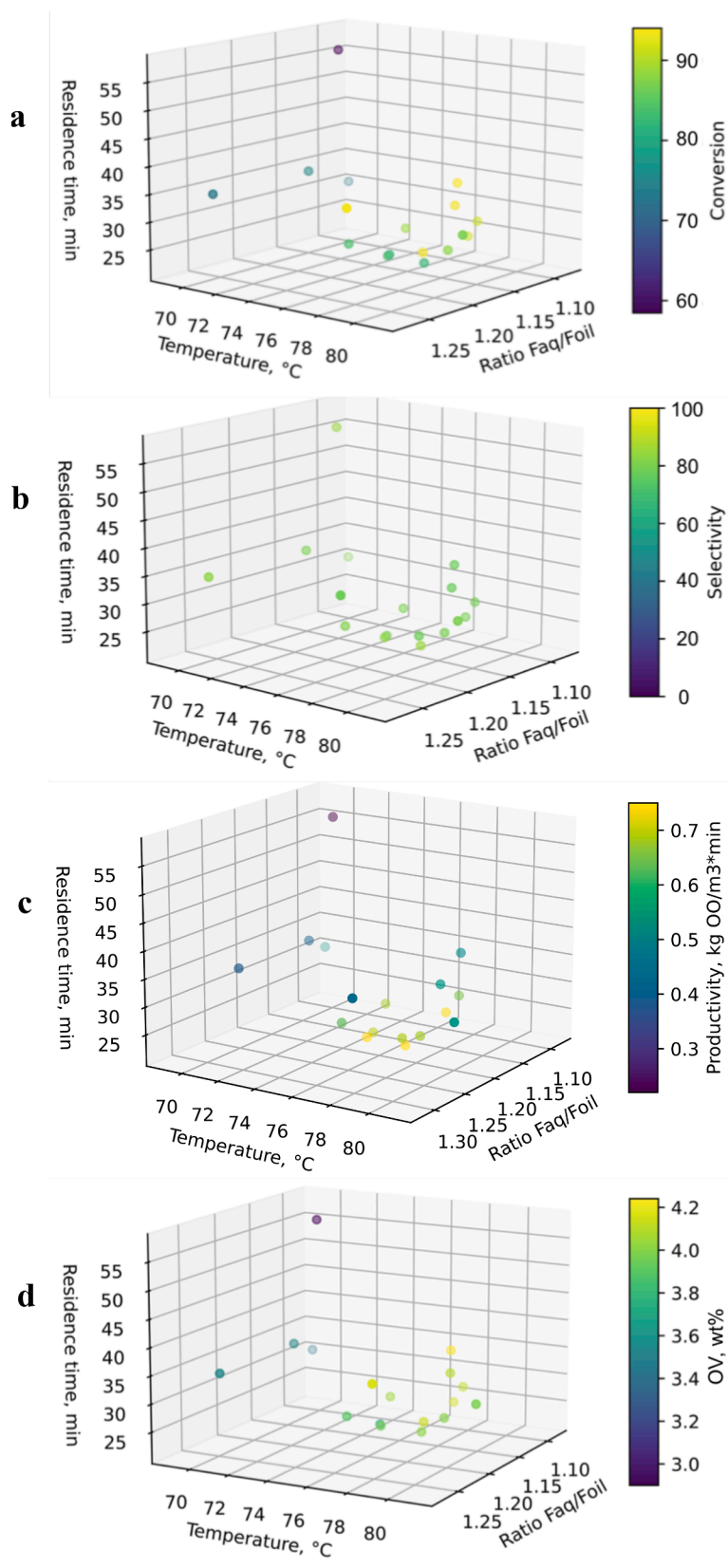


**Fig. 8.** Experimental results were obtained during the optimization of the slug flow reactor in the epoxidation of UCO using the simplex evolutionary algorithm. (a) Conversion. (b) Selectivity. (c) Productivity. (d) Oxirane oxygen content. Ratio  $F_{aq}/F_{oil}$  is the volumetric flow ratio between aqueous and oil phases.

Similarly, the standardized Pareto chart of Fig. S6 in the supplementary material indicates that temperature and residence time are statistically significant variables ( $p \leq 0.05$ ) affecting conversion. Specifically, conversion is strongly influenced by the volumetric flow ratios of acids to oil and  $\text{H}_2\text{O}_2$  to oil. By observing reported results in Table S3 and Fig. S5 in the supplementary material, it is clear that the high conversions of experiments 7 and 11, were obtained under the highest volumetric flow ratios for both acids to oil and  $\text{H}_2\text{O}_2$  to oil. These ratios are critical in epoxidation kinetics as they represent higher availability of the oxidizing agent and catalyst loadings, key factors in enhancing process efficiency.

Fig. 8b presents a three-dimensional space that describes the impact of assessed variables concerning selectivity towards oxirane groups. The selectivity ranged from 0.77 to 0.86 in all experiments, and despite the values are slightly lower than those obtained with pure soybean oil [34], these are in the range of those typically encountered in traditional batch epoxidation processes ( $\sim 0.80$ , [15,55]). Notably, most operating points were clustered at a higher selectivity range ( $> 0.80$ ), indicating that this variable was less affected than conversion at the different operating conditions. The standardized Pareto chart (Fig. S7 in the supplementary material) reveals that temperature is the only significant variable ( $p \leq 0.05$ ) influencing selectivity. This demonstrates the high-temperature control capability of the millireactor that mitigates thermally-driven ring-opening reactions, and the reliability of the slug flow reactor in producing consistent results in the epoxidation of UCOs.

The corresponding effects of the studied variables on reaction yield are presented in Fig. S5 and S8 in the supplementary material. This variable exhibited similar behavior to that observed in conversion, which can be attributed to selectivity presenting little variability under the evaluated operating conditions. The obtained values around the optimal conditions were  $\sim 0.71$ , below the previously observed in the epoxidation of soybean oil in the slug flow reactor ( $\sim 0.8$ , [34]). They were also lower than the obtained using commercial vegetable oils in traditional batch reactors (yield  $\sim 0.75$ ; [56]). This could be caused by the impurities on the raw material that affected reaction performance; polar compounds aided in boosting the penetration of water and acetic acid in the oil phase, thus triggering ring-opening reactions. Consequently, acetic acid was less available in the aqueous phase to form the peracetic acid that was the oxygen carrier to drive epoxidation. This result indicates that further explorations of the reactor could be focused primarily on optimizing reaction conversion and the corresponding productivity. This might involve tuning operating conditions in the slug flow reactor and implementing a better pretreatment process to reduce polar compounds of UCOs. Due to the low variability of selectivity, the significant variables affecting yield (Fig. S8 in the supplementary material) were the same as those affecting conversion.

In the case of reactor productivity, experimental data reveals a clear influence of the process variables, precisely temperature and residence time (Fig. 8c). The highest productivity ( $> 0.68 \text{ kg OO}\cdot\text{m}^{-3}\cdot\text{min}^{-1}$ ) was obtained at the higher operating temperatures (i.e.  $75.3 - 78.2^\circ\text{C}$ ) and at shorter residence times (around  $22.16 - 24.85 \text{ min.}$ ). This verifies that the process is operating in a kinetic regime that enables high epoxidation rates with good temperature control to avoid ring-opening reactions. Also, the low residence times obtained under higher flow rates enabled rapid removal of the epoxide, inhibiting further degradation. For similar reasons, the statistical analysis confirmed that the variable with the greatest impact on productivity is residence time (Fig. S9 in the supplementary material). Additionally, the volumetric flow ratio between the aqueous and oil phases was found to impact productivity, although less significantly than the effect of the other variables. The optimal productivity values were obtained within a narrow range ( $1.13 - 1.22$ ) of this flow ratio, suggesting the existence of an appropriate balance of mass transfer effectiveness, reactants ratio, and concentration of acid species.

The OV is a crucial variable in the epoxidation process, as it directly influences the ability of the product to meet the technical specifications

required for its intended applications. This metric determines the quality and degree of epoxidation of the oil, making it essential to optimize this property to ensure the performance and functionality of the epoxidized material. Fig. 8d illustrates the effect of residence time, temperature, and the volumetric flow rate ratio of the aqueous and oil phases on OV. The highest values (indicated by a yellowish color) were primarily observed under conditions of elevated temperatures ( $> 75.0^\circ\text{C}$ ) and shorter residence times (around  $25 \text{ min.}$ ). This again confirms that a proper trade-off between operating temperature and residence time leads to a more efficient epoxidation process. These results are also corroborated by the Pareto analysis (Fig. S10 in the supplementary material), where the statistically significant variables for oxirane value are temperature and residence time.

As a result of the optimization process, it was possible to identify the most suitable operating conditions to maximize productivity, selectivity, and conversion in the epoxidation process. Experiment 16 yielded the most favorable results, achieving a productivity of  $0.75 \text{ kg OO}\cdot\text{m}^{-3}\cdot\text{min}^{-1}$ , a conversion of  $82\%$ , a selectivity of  $86\%$ , and an oxirane index of  $4.02\%$  by weight. These optimal conditions were attained at a temperature of  $77.4^\circ\text{C}$ , with a residence time of  $22.16 \text{ min}$ , and with volumetric flow ratios of  $0.32:1$  for the acidity/oil and  $0.88:1$  for the  $\text{H}_2\text{O}_2$ /oil. These results are comparable to those previously reported in the same millireactor used in the epoxidation of soybean oil ( $X = 90\%$ ,  $S = 91\%$ ,  $P = 0.95 \text{ kg OO}\cdot\text{m}^{-3}\cdot\text{min}^{-1}$ ) [34]). On the other hand, the productivity achieved with UCOs ( $0.75 \text{ kg OO}\cdot\text{m}^{-3}\cdot\text{min}^{-1}$ ) and soybean oil ( $0.95 \text{ kg OO}\cdot\text{m}^{-3}\cdot\text{min}^{-1}$ ) in the millireactor of the present study was significantly higher compared to a similar flow reactor study using soybean oil, which achieved productivity of  $0.61 \text{ kg OO}\cdot\text{m}^{-3}\cdot\text{min}^{-1}$  [36]. Furthermore, when comparing the results obtained in the continuous millireactor with a fed-batch process, similar outcomes are observed regarding selectivity ( $71\%$ ) and total conversion. Nevertheless, considering productivity and residence time under optimal conditions, it is possible to verify the intensification of the process; the residence time was reduced from  $5$  to  $12 \text{ h}$  [57,15] to less than  $30 \text{ min}$ , and productivity was much larger ( $0.08 \text{ kg OO}\cdot\text{m}^{-3}\cdot\text{min}^{-1}$  to more than  $0.75 \text{ kg OO}\cdot\text{m}^{-3}\cdot\text{min}^{-1}$ ). Despite the promising results, further experiments must be carried out to assess the impact of UCOs physicochemical characteristics (i.e., polar compounds concentration, interfacial tension, and water content), and the potential benefits of specific pretreatment. Also, an assessment of the process with UCOs of higher unsaturation content would be of interest to produce epoxides with a higher oxirane oxygen content. Additionally, the obtained results would be helpful for further modeling and validation to conduct a feasibility assessment of the technology at larger scales.

#### 4. Conclusions

This research developed and optimized an automated platform for the continuous epoxidation of used cooking oils utilizing segmented flow milli-reactors. A detailed analysis of process variables found that viscosity plays a major role in achieving slug flow patterns, so specific operating conditions must be determined for different potential feedstocks. The high content of impurities, particularly of polar compounds, represents a major challenge for the proper hydrodynamic behavior of the slug flow reactor. Such impurities induce coalescence of the immiscible phases during epoxidations, reducing mass transfer area and affecting epoxidation effectiveness. Then, the humidity content and the presence of polar compounds could serve as indicators to assess whether a specific UCO is suitable as feedstock for slug flow reactors or if pretreatment is necessary. Nevertheless, it was possible to identify an appropriate range of operating conditions to produce the intended slug flow regime and carry out effective epoxidation.

By exploring the effect of temperature, residence time, and volumetric flow ratios between the aqueous and oil phases, optimal conditions that maximized productivity and yield of epoxidation in the millireactor were identified. The results demonstrated that high

temperatures (~ 77–80 °C) and shorter residence times (approximately 25–30 min.) were critical factors to obtain high conversion and productivity and to promote the formation of epoxidized compounds with high oxirane values. Under optimal conditions, a conversion of 82 % and a selectivity of 86 % were achieved in the epoxidation of used cooking oil. However, the evaluated millireactor exhibited superior productivity (0.75 kg OO·m<sup>-3</sup>·min<sup>-1</sup>) compared to previous studies using refined vegetable oils. Furthermore, similar outcomes were observed regarding selectivity, conversion, and yield when compared with a traditional fed-batch epoxidation process. The high productivity and low residence time confirmed the intensification of the process. This demonstrates that a continuous slug-flow millireactor can effectively reach high conversions, avoiding ring-opening degradation and minimizing unwanted byproducts that would affect the performance of the epoxidized UCO as a plasticizer. It is expected that it would be possible to scale up the process by using a combination of multiple millireactors of increased size. In this direction, the results would be valuable in constructing and validating computational models for process scale-up and further feasibility assessment.

### CRedit authorship contribution statement

**Juliana Cárdenas:** Writing – review & editing, Writing – original draft, Methodology, Investigation, Formal analysis, Data curation. **Benjamin Katryniok:** Writing – review & editing, Writing – original draft, Supervision, Resources, Funding acquisition. **Marcia Araque:** Writing – review & editing, Writing – original draft, Supervision, Formal analysis. **Wei-Hsin Hsu:** Writing – review & editing, Investigation. **Peter H. Seeberger:** Resources, Funding acquisition. **Jose Danglad-Flores:** Writing – review & editing, Writing – original draft, Supervision, Resources, Formal analysis, Conceptualization. **Alvaro Orjuela:** Writing – review & editing, Writing – original draft, Supervision, Resources, Project administration, Methodology, Investigation, Funding acquisition, Formal analysis, Conceptualization.

### Declaration of competing interest

The authors declare that they have no known competing financial interests or personal relationships that could have appeared to influence the work reported in this paper.

### Acknowledgements

This project was partially funded by the program ECOSNORD corresponding to Minciencias Contract 487-2021 and Minciencias Contract 933-2023. Juliana Cárdenas gratefully acknowledges financial support of the DAAD research scholarship - One-Year Grants for Doctoral Candidates, 2023/2024 (57645447). Dr. Jose Danglad Flores and Peter H. Seeberger thank the Max-Planck Society for generous funding.

### Appendix A. Supplementary data

Supplementary data to this article can be found online at <https://doi.org/10.1016/j.cej.2025.159907>.

### Data availability

Data will be made available on request.

### References

- [1] W.H. Foo, S.S.N. Koay, S.R. Chia, W.Y. Chia, D.Y.Y. Tang, S. Nomanbhay, K. W. Chew, Recent advances in the conversion of waste cooking oil into value-added products: a review, *Fuel* 324 (Part A) (2022), <https://doi.org/10.1016/j.fuel.2022.124539>.
- [2] C.S.K. Lin, L.A. Pfaltzgraff, L. Herrero-Davila, E.B. Mubofu, S. Abderrahim, J. H. Clark, A.A. Koutinas, N. Kopsahelis, K. Stamatelatu, F. Dickson, R. Brocklesby, R. Luque, Food waste as a valuable resource for the production of chemicals, materials and fuels. Current situation and global perspective, *Energ. Environ. Sci.* 6 (2) (2013) 426–464, <https://doi.org/10.1039/c2ee23440h>.
- [3] A. Orjuela, J. Clark, Green chemicals from used cooking oils: Trends, challenges, and opportunities, *Curr. Opin. Green Sustainable Chem.* 26 (2020) 100369, <https://doi.org/10.1016/j.cogsc.2020.100369>.
- [4] Trivedi, J., Bhonsle, A. K., Atray, N. 2019. Processing food waste for the production of platform chemicals. In: Kumar, R. P., Gnansounou, E., Raman, J. K., Baskar, G. (Eds.) *Refining Biomass Residues for Sustainable Energy and Bioproducts: Technology, Advances, Life Cycle Assessment, and Economics*. doi: 10.1016/B978-0-12-818996-2.00019-3.
- [5] J. Cárdenas, A. Orjuela, D.L. Sánchez, P.C. Narváez, B. Katryniok, J. Clark, Pretreatment of used cooking oils for the production of green chemicals: a review, *J. Clean. Prod.* 289 (2021) 125129, <https://doi.org/10.1016/j.jclepro.2020.125129>.
- [6] G. Bansal, W. Zhou, P.J. Barlow, P.S. Joshi, H.L. Lo, Y.K. Chung, Review of rapid tests available for measuring the quality changes in frying oils and comparison with standard methods, *Crit. Rev. Food Sci. Nutr.* 50 (6) (2010) 503–514, <https://doi.org/10.1080/10408390802544611>.
- [7] S. Marmesat, E. Rodrigues, J. Velasco, C. Dobarganes, Quality of used frying fats and oils: comparison of rapid tests based on chemical and physical oil properties, *Int. J. Food Sci. Technol.* 42 (5) (2007) 601–608, <https://doi.org/10.1111/j.1365-2621.2006.01284.x>.
- [8] J. Cvengroš, Z. Cvengrošová, Used frying oils and fats and their utilization in the production of methyl esters of higher fatty acids, *Biomass Bioenergy* 27 (2) (2004) 173–181, <https://doi.org/10.1016/j.biombioe.2003.11.006>.
- [9] C.G. Lopresto, M.G. De Paola, V. Calabrò, Importance of the properties, collection, and storage of waste cooking oils to produce high-quality biodiesel – an overview, *Biomass Bioenergy* 189 (2024) 107363, <https://doi.org/10.1016/j.biombioe.2024.107363>.
- [10] T.D. Tsoutsos, S. Tournaki, O. Paraífa, S.D. Kaminaris, The Used Cooking Oil-to-biodiesel chain in Europe assessment of best practices and environmental performance, *Renew. Sustain. Energy Rev.* 54 (2016) 74–83, <https://doi.org/10.1016/j.rser.2015.09.039>.
- [11] Z. Yaakob, M. Mohammad, M. Alherbawi, Z. Alam, K. Sopian, Overview of the production of biodiesel from Waste cooking oil, *Renew. Sustain. Energy Rev.* 18 (2013) 184–193, <https://doi.org/10.1016/j.rser.2012.10.016>.
- [12] Arkema. 2014. Vikoflex® 7170 Epoxidized Soybean Oil Data Sheet. Online. Available at: <https://www.yumpu.com/en/document/read/15650446/vikoflexr-7170-arkema-inc> Accessed Nov, 2024.
- [13] C. Cai, H. Dai, R. Chen, C. Su, X. Xu, S. Zhang, L. Yang, Studies on the kinetics of in situ epoxidation of vegetable oils, *Eur. J. Lipid Sci. Technol.* 110 (4) (2008) 341–346, <https://doi.org/10.1002/ejlt.200700104>.
- [14] Y. Ma, Y. Hu, Y. Fang, Q. Li, Q. Huang, Q. Shang, M. Zhang, S. Li, P. Jia, Y. Zhou, Recent advances in vegetable oil based fine chemicals and polymers, *Green Mater.* (2024) 1–22, <https://doi.org/10.1680/jgrma.24.00083>.
- [15] T. Cogliano, R. Turco, M. Di Serio, T. Salmi, R. Tesser, V. Russo, Epoxidation of vegetable oils via the prilezhaev reaction method: a review of the transition from batch to continuous processes, *Ind. Eng. Chem. Res.* 63 (26) (2024) 11231–11262, <https://doi.org/10.1021/acs.iecr.3c04211>.
- [16] S.M. Danov, O.A. Kazantsev, A.L. Esipovich, A.S. Belousov, A.E. Rogozhin, E. A. Kanakov, Recent advances in the field of selective epoxidation of vegetable oils and their derivatives: a review and perspective, *Cat. Sci. Technol.* 7 (17) (2017) 3659–3675, <https://doi.org/10.1039/c7cy00988g>.
- [17] S. Leveneur, P. Tolvanen, V. Russo, Catalytic epoxidation reaction, *Catalysts* 14 (5) (2024) 285, <https://doi.org/10.3390/catal14050285>.
- [18] M. Kurańska, M. Niemiec, Cleaner production of epoxidized cooking oil using a heterogeneous catalyst, *Catalysts* 10 (11) (2020) 1261, <https://doi.org/10.3390/catal10111261>.
- [19] M.S. Bhalerao, V.M. Kulkarni, A.V. Patwardhan, Ultrasound-assisted chemoenzymatic epoxidation of soybean oil by using lipase as biocatalyst, *Ultrason. Sonochem.* 40 (Part A) (2018) 912–920, <https://doi.org/10.1016/j.ulsonch.2017.08.042>.
- [20] N. Sarmah, V. Mehtab, K. Borah, A. Palanisamy, R. Parthasarathy, S. Chenna, Inverse design of chemoenzymatic epoxidation of soybean oil through artificial intelligence-driven experimental approach, *Bioresour. Technol.* 412 (2024) 131405, <https://doi.org/10.1016/j.biortech.2024.131405>.
- [21] S.K. Maiti, W.K. Snavely, P. Venkatasubramanian, E.C. Hagberg, D.H. Busch, B. Subramaniam, Reaction engineering studies of the epoxidation of fatty acid methyl esters with venturrello complex, *Ind. Eng. Chem. Res.* 58 (7) (2019) 2514–2523, <https://doi.org/10.1021/acs.iecr.8b05977>.
- [22] Z.P. Pai, Y.A. Chesalov, P.V. Berdnikova, E.A. UsLamin, D.Y. Yushchenko, Y. V. Uchenova, T.B. Khlebnikova, V.P. Baltakhinov, D.I. Kochubey, V.I. Bukhtiyarov, Tungsten peroxopolyoxo complexes as advanced catalysts for the oxidation of organic compounds with hydrogen peroxide, *Appl. Catal. A* 604 (2020) 117786, <https://doi.org/10.1016/j.apcata.2020.117786>.
- [23] J. Cárdenas, B. Katryniok, M. Araque, A. Orjuela, Synthesis of a modified heteropolyacid and evaluation as a phase-transfer catalyst for soybean oil epoxidation, *Chem. Eng. Res. Des.* 211 (2024) 356–366, <https://doi.org/10.1016/j.cherd.2024.10.010>.
- [24] M. Hegelmann, W.F. Bohórquez, J. Luibl, A. Jess, A. Orjuela, M. Cokoja, Biphasic phase-transfer catalysis: epoxidation of vegetable oils by surface active ionic liquids in water, *React. Chem. Eng.* 14 (2024) 1–7, <https://doi.org/10.1039/D4RE00215F>.

- [25] F. Zhang, Y. Dong, S. Lin, X. Gui, J. Hu, A novel amphiphilic phase transfer catalyst for the green epoxidation of soybean oil with hydrogen peroxide, *Mol. Catal.* 547 (2023) 113384, <https://doi.org/10.1016/j.mcat.2023.113384>.
- [26] B.M. Abdullah, J. Salimon, Epoxidation of vegetable oils and fatty acids: Catalysts, methods and advantages, *J. Appl. Sci.* 10 (15) (2010) 1545–1553, <https://doi.org/10.3923/jas.2010.1545.1553>.
- [27] J. La Scala, R.P. Wool, Effect of FA composition on epoxidation kinetics of TAG, *JAOCs, J. Am. Oil Chemists' Soc.* 79 (4) (2002) 373–378, <https://doi.org/10.1007/s11746-002-0491-9>.
- [28] B. Rangarajan, A. Havey, E.A. Grulke, P.D. Culnan, Kinetic parameters of a two-phase model for in situ epoxidation of soybean oil, *J. Am. Oil Chemists' Soc.* 72 (10) (1995) 1161–1169, <https://doi.org/10.1007/BF02540983>.
- [29] P. Miéville, F. de Nanteuil, Modern Automation in Organic Synthesis Laboratories, in: Reference Module in Chemistry, Molecular Sciences and Chemical Engineering, Elsevier, Amsterdam, The Netherlands, 2024, <https://doi.org/10.1016/B978-0-323-96025-0.00047-8>.
- [30] M. Seifrid, R. Pollice, A. Aguilar-Granda, Z. Morgan Chan, K. Hotta, C.T. Ser, J. Vestfrid, T.C. Wu, A. Aspuru-Guzik, Autonomous chemical experiments: challenges and perspectives on establishing a self-driving lab, *Acc. Chem. Res.* 55 (17) (2022) 2454–2466, <https://doi.org/10.1021/acs.accounts.2c00220>.
- [31] P. Lutze, R. Gani, J.M. Woodley, Process intensification: a perspective on process synthesis, *Chem. Eng. Process.* 49 (6) (2010) 547–558, <https://doi.org/10.1016/j.cep.2010.05.002>.
- [32] J.M. Ponce-Ortega, M.M. Al-Thubaiti, M.M. El-Halwagi, Process intensification: new understanding and systematic approach, *Chem. Eng. Process.* 53 (2012) 63–75, <https://doi.org/10.1016/j.cep.2011.12.010>.
- [33] A. Stankiewicz, T.V. Gerven, G. Stefanidis, *The Fundamentals of Process Intensification*, 1st Ed., Wiley-VCH, Weinheim, Germany, 2019.
- [34] Cárdenas, J., Katryniok, B., Araque, M., Seeburger, P. H., Danglad-Flores, J., Orjuela, A. 2025. Intensified Epoxidation of Soybean Oil: Evaluation and Experimental Optimization in a Slug-Flow Millireactor. *Chemical Engineering Journal*. In Revision.
- [35] G.V. Olivieri, R. Giudici, CFD and reaction aspects for the soybean oil epoxidation in a millireactor, *Chem. Eng. Process. - Process Intensif.* 193 (2023) 109557, <https://doi.org/10.1016/j.cep.2023.109557>.
- [36] G.V. Olivieri, P.A. Meira, T.T. de Mattos, H.M. Okuda, J.V. de Quadros, M.S. A. Palma, R. Giudici, Microreactor x millireactor: Experimental performance in the epoxidation of soybean oil, *Chem. Eng. Process. - Process Intensif.* 193 (2023) 109562, <https://doi.org/10.1016/j.cep.2023.109562>.
- [37] M.N. Kashid, I. Gerlach, S. Goetz, J. Franzke, J.F. Acker, F. Platte, D.W. Agar, S. Turek, Internal circulation within the liquid slugs of a liquid-liquid slug-flow capillary microreactor, *Ind. Eng. Chem. Res.* 44 (14) (2005) 5003–5010, <https://doi.org/10.1021/ie0490536>.
- [38] J. Zhang, K. Wang, A.R. Teixeira, K.F. Jensen, G. Luo, Design and scaling up of microchemical systems: a review, *Annu. Rev. Chem. Biomol. Eng.* 8 (2017) 285–305, <https://doi.org/10.1146/annurev-chembioeng-060816-101443>.
- [39] X. Wang, Y. Wang, F. Li, L. Li, X. Ge, S. Zhang, T. Qiu, Scale-up of microreactor: Effects of hydrodynamic diameter on liquid-liquid flow and mass transfer, *Chem. Eng. Sci.* 226 (2020) 115838, <https://doi.org/10.1016/j.ces.2020.115838>.
- [40] Z. Dong, Z. Wen, F. Zhao, S. Kuhn, T. Noël, Scale-up of micro- and millireactors: an overview of strategies, design principles and applications, *Chem. Eng. Sci.* X 10 (2021) 100097, <https://doi.org/10.1016/j.cesx.2021.100097>.
- [41] Ehrfeld. 2022. Integrated scale-up concept. Ehrfeld Mikrotechnik GmbH. Online. Available at: <https://www.ehrfeld.com/en/labor-integriertes-scale-up-konzept> Accessed Jan. 2025.
- [42] L.A. Rincón, J. Cárdenas, A. Orjuela, Used cooking oils as potential oleochemical feedstock for urban biorefineries – Study case in Bogota, Colombia, *Waste Manag.* 88 (2019) 200–210, <https://doi.org/10.1016/j.wasman.2019.03.042>.
- [43] GitHub. 2022. GitHub – cambiegroup/flowchem: Flowchem is an application to simplify the control of instruments and devices commonly found in chemistry labs. <https://github.com/cambiegroup/flowchem>.
- [44] W. Spendley, G.R. Hext, F.R. Himsforth, Sequential application of simplex designs in optimisation and evolutionary operation, *Technometrics* 4 (4) (1962) 441–461, <https://doi.org/10.1080/00401706.1962.10490033>.
- [45] J. Cárdenas, M.A. Montañez, A. Orjuela, P.C. Narváez, B. Katryniok, Deacidification of used cooking oils by solvent extraction under lab scale and in a falling film contactor, *Chem. Eng. Process. - Process Intensif.* 181 (2022) 109089, <https://doi.org/10.1016/j.cep.2022.109089>.
- [46] T. Eryilmaz, F. Aksoy, L. Aksoy, H. Bayrakceken, F.E. Aysal, S. Sahin, M. K. Yesilyurt, Process optimization for biodiesel production from neutralized waste cooking oil and the effect of this biodiesel on engine performance, *CTyF - Ciencia, Tecnologia y Futuro* 8 (1) (2018) 121–127, <https://doi.org/10.29047/01225383.99>.
- [47] A.S. Ramadhas, S. Jayaraj, C. Muraleedharan, Biodiesel production from high FFA rubber seed oil, *Fuel* 84 (4) (2005) 335–340, <https://doi.org/10.1016/j.fuel.2004.09.016>.
- [48] W.F. Bohórquez, A. Orjuela, P.C. Narváez, J.G. Cadavid, J.A. García-Nunez, Experimental optimization during epoxidation of a high-oleic palm oil using a simplex algorithm, *Ind. Crop. Prod.* 187PA (2022) 115321, <https://doi.org/10.1016/j.indcrop.2022.115321>.
- [49] Tarmizi, A. H., Samsul, K. R., Zaiton, R., Rosli, M. Y. 2008. Multiplication of oil palm liquid cultures in bioreactors. *J. Oil Palm Res.*, 20, No. April, 44-50 ref. 22. <https://palmoilis.mpob.gov.my/publications/jopr2008sp-ms44.pdf>.
- [50] FAO. 1999. Codex Standards for Fats and Oils from Vegetable Sources - Standard for named vegetable oils CODEX STAN 210-1999. ALIMENTARIUM, C. Online. Available at: [https://www.fao.org/input/download/standards/336/CXS\\_210e\\_2015.pdf](https://www.fao.org/input/download/standards/336/CXS_210e_2015.pdf) Accessed Nov, 2024.
- [51] L. Xu, F. Yang, X. Li, C. Zhao, Q. Jin, J. Huang, X. Wang, Kinetics of forming polar compounds in frying oils under frying practice of fast food restaurants, *LWT* 115 (2019) 108307, <https://doi.org/10.1016/j.lwt.2019.108307>.
- [52] L.A. Rincón, J.G. Cadavid, A. Orjuela, Assessment of degumming and bleaching processes for used cooking oils upgrading into oleochemical feedstocks, *J. Environ. Chem. Eng.* 9 (1) (2021) 104610, <https://doi.org/10.1016/j.jece.2020.104610>.
- [53] L.M. Ramírez, J.G. Cadavid, A. Orjuela, M.F. Gutiérrez, W.F. Bohórquez, Epoxidation of used cooking oils: Kinetic modeling and reaction optimization, *Chem. Eng. Process. - Process Intensif.* 176 (2022) 108963, <https://doi.org/10.1016/j.cep.2022.108963>.
- [54] Stewart, M. 2016. Fluid flow and pressure drop. In: *Surface Production Operations*, 343–470. Elsevier. Elsevier. The Netherlands. doi: 10.1016/b978-1-85617-808-2.00006-7.
- [55] S. Dinda, A.V. Patwardhan, V.V. Goud, N.C. Pradhan, Epoxidation of cottonseed oil by aqueous hydrogen peroxide catalysed by liquid inorganic acids, *Bioresour. Technol.* 99 (9) (2008) 3373–3744, <https://doi.org/10.1016/j.biortech.2007.07.015>.
- [56] A. Guo, Z. Petrovic, Vegetable Oils-Based Polyols, in: S.Z. Erhan (Ed.), *Industrial Uses of Vegetable Oil*, AOCS Publishing, NY, USA, 2005, <https://doi.org/10.4324/9781003040248>.
- [57] A. Campanella, C. Fontanini, M.A. Baltanás, High yield epoxidation of fatty acid methyl esters with performic acid generated in situ, *Chem. Eng. J.* 144 (3) (2008) 466–475, <https://doi.org/10.1016/j.cej.2008.07.016>.